Article ID：1007−7294(2025)06−0878−10

Numerical Modeling of Ship-Ice-Water Interaction for Free-running Ships in Pack Ice

ZOU Ming [1a,2], *ZOU Zao−jian* [1a,1b], *ZOU Lu* [1a,1b], *ZHU Sheng−tao* [1a]

(1a. School of Ocean and Civil Engineering; b. State Key Laboratory of Ocean Engineering, Shanghai Jiao Tong University, Shanghai 200240, China; 2. Marine Design and Research Institute of China, Shanghai 200011, China)

Abstract: Ice-going ships play a crucial role in polar transportation and resource extraction. Different from the existing modeling approach which assumes that ships remain stationary, dynamic overset grid technology and DFBI (Dynamic Fluid-Body Interaction) method are employed in this paper to enable the free-running motion of the ship in modeling. A numerical model capable of simulating a ship navigating through pack ice area is proposed, which uses Computational Fluid Dynamics (CFD) method to solve the flow field and applies the Discrete Element Method (DEM) to simulate ship-ice and ice-ice interactions. Besides, the proposed high-precision method for generating pack ice area can be used in conjunction with the proposed numerical model. By comparing the numerical results with the available model test data and experimental observations, the effectiveness of the numerical model is validated, demonstrating its strong capability of predicting resistance and simulating ship navigation in pack ice, as well as its significant potential and applicability for further studies.

Key words: pack ice; ship-ice-water interaction; CFD–DEM; dynamic overset grid technology; ship resistance

CLC number: U661.31+1 **Document code:** A **doi:** 10.3969/j.issn.1007−7294.2025.06.003

0 Introduction

The ice resistance performance of ice-going ships is directly related to their navigation efficiency and economic viability, serving as a crucial basis for designing and optimizing their hull form. Most of the existing studies on the ice resistance of ice-going ships are conducted under level ice condition[1−2]. However, as the effects of global warming persist and the Arctic route continues to develop, the pack ice condition is likely to become the most common environment for future polar transportation[3−4]. Therefore, it is necessary to conduct study specifically targeting pack ice condition.

In the study of ship-ice interaction in pack ice, experimental and numerical methods are commonly used. Compared to experimental methods[5−7], numerical methods are advantageous because they are of lower costs, capable of controlling the variables involved and being implemented during the ship design phase. Løset[8] used the two-dimensional disc Discrete Element Method（DEM）to construct a pack ice area and employed a

Received date：2024−12−26

Foundation item：Supported by the National Key Laboratory of Science and Technology on Hydrodynamics (Grant No. 2022-JCJQ-LB-028)

Biography：ZOU Ming(1995–), male, Ph.D. candidate; ZOU Zao-jian(1956–), male, professor, Ph.D. supervisor, corresponding author, E-mail: zjzou@sjtu.edu.cn; ZOU Lu(1983–), female, associate professor, Ph.D. supervisor; ZHU Sheng-tao(2000–), male, master student.

linear viscoelastic model to simulate ice collisions. Wang et al.[9] used the Finite Element Method（FEM）to simulate the navigation of an ice-going ship in pack ice area, and compared the numerical results with experimental data to validate the reliability of the numerical method. As the study progresses, the influence of flow field and ship-generated waves on ship-ice interactions has been taken into consideration. To solve the more complex ship-ice-water coupling problems, Vroegrijk[10] proposed a CFD-DEM method that couples the flow field with the ice field, employing CFD（Computational Fluid Dynamics）to simulate the flow field and DEM to simulate the ship-ice and ice-ice interactions. Compared to other numerical methods, this method effectively integrates the advantages of CFD in fluid flow analysis, enabling a more realistic representation of ship-ice-water interaction[11−12]. It has become a popular method for studying ice resistance of ships navigating in pack ice in recent years. Some researchers have applied this method and achieved some good results[13−16].

In the existing studies based on the CFD-DEM method, ships are commonly assumed to be stationary. The relative motion between the ship, the pack ice and water is achieved by the steady motion of the pack ice and water towards the ship at a speed equal to the ship speed. However, when modeling in this way, the velocity of pack ice may change due to the influence of other pack ice and the flow field before the pack ice encounters the ship, resulting in inconsistencies between the encountering velocity and the given velocity[13]. To address this issue and enrich research means, a numerical model is proposed in this paper that allows ships to navigate through pack ice in free-running motion, along with a high-precision method for generating pack ice area to be used in conjunction with this model.

1 Numerical method

1.1 Governing equations of fluid flow

The solution of the fluid flow is obtained by solving the Reynolds-averaged continuity equation and the Reynolds-averaged Navier-Stokes（RANS）equations for an incompressible Newtonian fluid:

$$\nabla \cdot \overline{\boldsymbol{u}} = 0 \tag{1}$$

$$\frac{\partial(\rho_{\mathrm{f}}\overline{\boldsymbol{u}})}{\partial t} + \nabla \cdot (\rho_{\mathrm{f}}\overline{\boldsymbol{u}}\overline{\boldsymbol{u}}) = -\nabla \overline{p} + \nabla \cdot \left(\overline{\tau} - \rho_{\mathrm{f}}\overline{\boldsymbol{u}'\boldsymbol{u}'}\right) + \rho_{\mathrm{f}}\mathbf{g} \tag{2}$$

where $\overline{\boldsymbol{u}}$ is the time-averaged velocity, $\bar{p}$ is the time-averaged pressure of the fluid, ρ_{f} is the mass density, $\bar{\tau}$ is the viscous stress term, $\boldsymbol{g}$ is the gravitational acceleration, and $-\rho_f\overline{\boldsymbol{u}'\boldsymbol{u}'}$ is the Reynolds stress term.

1.2 Governing equations of pack ice motion

The motion of discrete pack ice in ship-ice-water interaction includes translational motion and rotational motion. The governing equations are as follows:

$$m_i\frac{\mathrm{d}v_i}{\mathrm{d}t} = \boldsymbol{F}_{\mathrm{g}} + \boldsymbol{F}_{\mathrm{c}} + \boldsymbol{F}_{\mathrm{f}} \tag{3}$$

$$\boldsymbol{I}_i\frac{\mathrm{d}\omega_i}{\mathrm{d}t} = \boldsymbol{M}_{\mathrm{c}} + \boldsymbol{M}_{\mathrm{f}} \tag{4}$$

where m_i and $\boldsymbol{v}_i$ are the mass and velocity of the i-th discrete pack ice; $\boldsymbol{F}_{\mathrm{g}}$, $\boldsymbol{F}_{\mathrm{c}}$, and $\boldsymbol{F}_{\mathrm{f}}$ are the gravity, the contact force, and the force acting on the i-th discrete pack ice by the fluid, respectively; I_i and $\boldsymbol{\omega}_i$ are the moment of inertia and the angular velocity; $\boldsymbol{M}_c$ is the total moment from contact forces, and $\boldsymbol{M}_f$ is the moment acting on the i-th discrete pack ice by the fluid.

The contact force $\boldsymbol{F}_{\mathrm{c}}$ can be expressed as

$$\boldsymbol{F}_{\mathrm{c}} = \boldsymbol{F}_{\mathrm{n}} + \boldsymbol{F}_{\mathrm{t}} \tag{5}$$

where $\boldsymbol{F}_{\mathrm{n}}$ is the normal contact force and $\boldsymbol{F}_{\mathrm{t}}$ is the tangential contact force, which can be expressed as

$$\boldsymbol{F}_{\mathrm{n}} = -K_{\mathrm{n}}\boldsymbol{d}_{\mathrm{n}} - N_{\mathrm{n}}\boldsymbol{v}_{\mathrm{n}} \tag{6}$$

$$\boldsymbol{F}_{\mathrm{t}}=\begin{cases}-K_{\mathrm{t}}\boldsymbol{d}_{\mathrm{t}}-N_{\mathrm{t}}v_{\mathrm{t}}, & |K_{\mathrm{t}}\boldsymbol{d}_{\mathrm{t}}|<|K_{\mathrm{n}}\boldsymbol{d}_{\mathrm{n}}|C_{\mathrm{fs}}\\ \dfrac{|K_{\mathrm{n}}\boldsymbol{d}_{\mathrm{n}}|C_{\mathrm{fs}}\boldsymbol{d}_{\mathrm{t}}}{|\boldsymbol{d}_{\mathrm{t}}|}, & |K_{\mathrm{t}}\boldsymbol{d}_{\mathrm{t}}|>|K_{\mathrm{n}}\boldsymbol{d}_{\mathrm{n}}|C_{\mathrm{fs}}\end{cases} \tag{7}$$

where K_{n} is the normal spring stiffness, $\boldsymbol{d}_{\mathrm{n}}$ is the overlap in the normal direction, N_{n} is the normal damping, $\boldsymbol{v}_{\mathrm{n}}$ is the normal velocity component, K_{t} is the tangential spring stiffness, $\boldsymbol{d}_{\mathrm{t}}$ is the overlap in the tangential direction, N_{t} is the tangential damping, $\boldsymbol{v}_{\mathrm{t}}$ is the tangential velocity component, and C_{fs} is the static friction coefficient.

1.3 CFD-DEM coupling scheme

Currently, there are two coupling schemes for CFD-DEM: one-way coupling scheme and two-way coupling scheme. The one-way coupling scheme only considers the influence of fluid on discrete pack ice, while the two-way coupling scheme considers the mutual influence of fluid and discrete pack ice. The existing study results indicate that there is no significant difference in predicting ice resistance between the one-way and two-way coupling schemes[17−18]. However, the one-way coupling scheme offers higher computational efficiency. Therefore, the one-way coupling scheme is adopted in this study.

1.4 Dynamic overset grid technology

In this paper, the dynamic overset grid technology combined with the DFBI（Dynamic Fluid-Body Interaction）module is applied to simulate the free-running motion of the ship. Applying this technology, the computational domain is divided into two parts: the overset domain and the background domain. Within the background domain, mesh cells are categorized into active, inactive, and acceptor cells. Active cells are those where the discretized governing equations of fluid flow are solved. Inactive cells are those where no equations are solved, yet they can become active as the overset domain shifts. Acceptor cells, positioned at the overset interface, primarily serve to distinguish between active and inactive cells.

2 Study objects

2.1 Ship model

The ship model used in this study is a model of the 76 000 DWT ice-strengthened Panamax bulker, which was used in the concerned model test[19]. The geometry of the hull is shown in Fig. 1. The scale ratio is 1: 45, and the main particulars of the ship are given in Tab. 1.

Fig.1 Geometry of the 76 000 DWT ice-strengthened Panamax bulker

Tab.1 Main particulars of the 76 000 DWT ice-strengthened Panamax bulker

Parameter	Symbol/Unit	Full scale	Model scale
Length of overall	L_{oa}/m	225	5.00
Length between perpendiculars	L_{PP}/m	217	4.82
Breadth	B/m	32.25	0.72
Depth	D/m	20.10	0.45
Designed draft	T/m	12.40	0.28

2.2 Pack ice model

In the model test[19] for comparison, paraffin model ice with six different sizes and a thickness of 0.02 m was used, without considering the breaking and cracking of pack ice. This study employs a composite particle model to simulate these six sizes of pack ice, similarly disregarding the breaking and cracking of pack ice. The modeled pack ice is shown in Fig. 2.

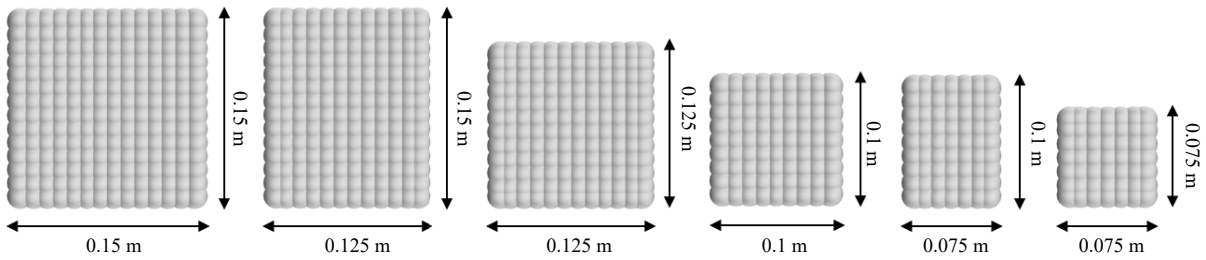

Fig.2 Pack ice models with different sizes in numerical simulation

The mass density of the pack ice model is 917 kg/m^3, and the Poisson's ratio is 0.30. The Young's modulus of the full-scale ice is 9 GPa[20]; correspondingly, the Young's modulus of the pack ice model in this study is 200 MPa through scale conversion. In addition to the parameters of pack ice, the contact parameters also have a direct impact on the ship-ice and ice-ice interactions. Referring to the parameter settings in the authors' previous studies[12,21], the static friction coefficients for ship-ice and ice-ice interactions are 0.40 and 0.10, respectively; the tangential and normal restitution coefficients are both 0.50.

3 Numerical setup

3.1 Computational domain and mesh generation

Fig. 3 illustrates the computational domain used in this study. The width of the computational domain is 7 m, consistent with that in the model test[19]. The total length of the computational domain is 57 m, with the length of the pack ice area being 21 m. The height of the computational domain is 14 m, with the air domain occupying a height of 5 m and the water domain occupying a height of 9 m.

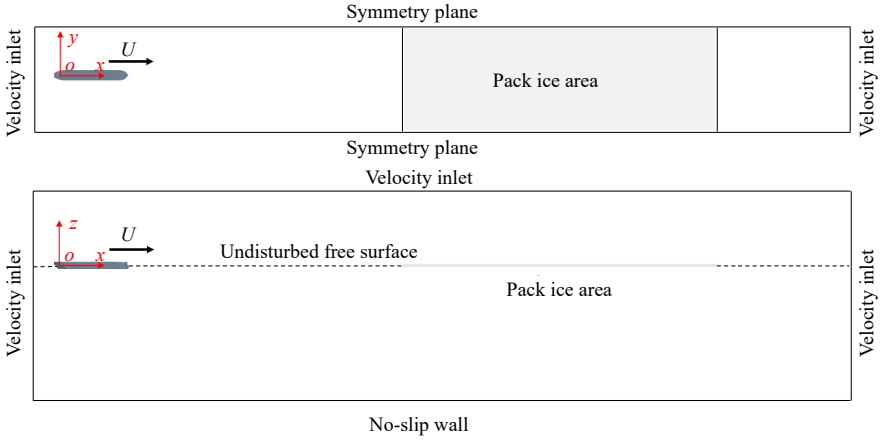

Fig.3 Computational domain and boundary conditions (Upper: top view; Lower: side view)

As shown in Fig. 3, the velocity inlet condition is applied on the inlet, outlet and top boundaries; and a symmetry plane condition is imposed on the side boundaries. On the hull surface and the bottom boundary,

non-slip wall condition is imposed. In addition, wave damping is set on the inlet and outlet boundaries to reduce the wave reflection from the boundaries.

The whole computational domain is discretized by the Trimmer Cell Mesher, as shown in Fig. 4. The meshes around the free surface are refined with multiple layers to capture the details of complex flow. To accurately resolve the flow in the boundary layer, the prism layer meshes are generated near the hull surface. Additionally, the meshes in the bow and stern regions are further refined to capture the flow characteristics in these specific areas, as shown in Fig. 4(c).

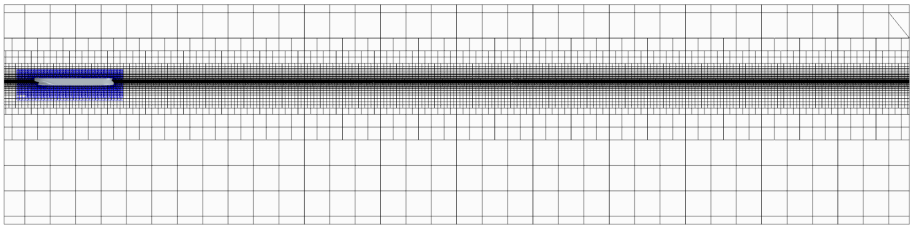

(a) Global meshes (Side view)

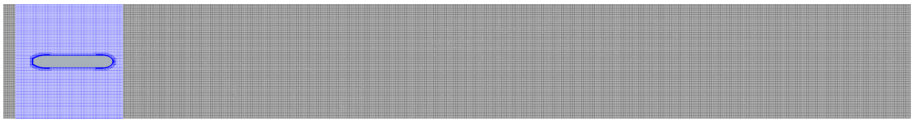

(b) Global meshes (Top view)

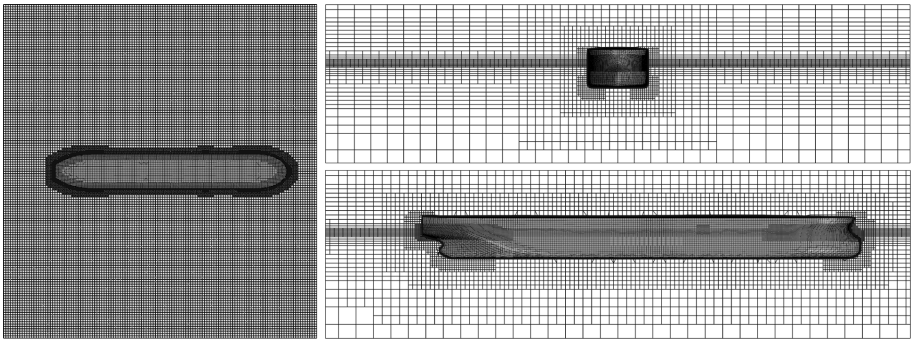

(c) Overset meshes (Left: top view; Upper right: back view; Lower right: side view)

Fig.4 Mesh distributions

3.2 Generation of pack ice

Different from the previous studies using CFD-DEM model where the ship remains stationary, in this study, the ship is in free-running motion. As a result, the pack ice area needs to be generated on the undisturbed free surface with high precision before numerical simulation. To this end, a method for generating pack ice area is proposed, with the following implementation steps:

(1) Establish the generation area: create a generation area that matches the intended size of the pack ice area to confine the range of pack ice generation;

(2) Determine the generation points: arrange generation points within the generation area to discretize it and to identify the locations for pack ice generation;

(3) Calculate and sort: calculate the quantities of pack ice of various sizes based on their distribution probabilities, and sort them to determine the generation order, prioritizing the generation of larger pack ice first;

(4) Search and generate: generate pack ice by searching the generation points. If the newly generated pack ice overlaps with the previously generated ones, the newly generated pack ice is removed, and the

generation points are searched again to complete the generation.

In numerical simulations, the distribution probability of different-sized pack ice is consistent with that of the model test[19], as shown in Tab. 2. Tab. 3 presents the comparison between the quantity of target pack ice and the generated pack ice in numerical simulations, along with the generation errors. Fig. 5 shows the pack ice area established using the pack ice generation method proposed in this study with the pack ice concentration $C = 60\%$.

Tab.2 Distribution probability of pack ice

Size/(m × m)	Probability
0.075 × 0.075	0.333
0.075 × 0.10	0.240
0.10 × 0.10	0.177
0.125 × 0.125	0.102
0.125 × 0.15	0.079
0.15 × 0.15	0.069

Tab.3 Error in the pack-ice generation

Size/(m × m)	Target quantity	Generated quantity	Error (%)	Average error (%)
0.075 × 0.075	2922	2927	0.17	0.77
0.075 × 0.10	2100	2110	0.48	
0.10 × 0.10	1550	1541	0.58	
0.125 × 0.125	897	885	1.34	
0.125 × 0.15	693	688	0.72	
0.15 × 0.15	602	610	1.33	

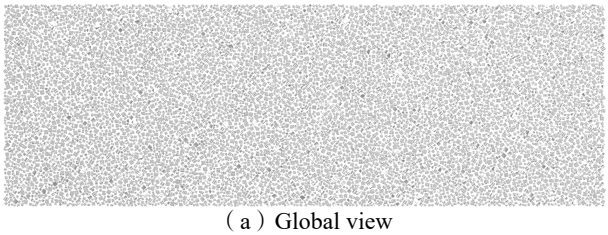

（a）Global view

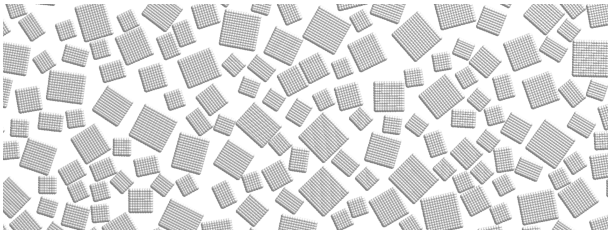

（b）Local view

Fig.5 Generated pack ice in numerical simulation ($C = 60\%$)

From Tab. 3, it can be seen that the generation error of pack ice is extremely small, with the maximum generation error less than 2%, and the average error less than 1%. This indicates that the pack ice generation method proposed in this study has high precision. Additionally, as shown in Fig. 5, the generated pack ice has random initial angles and remains stationary on the undisturbed free surface, indicating the effectiveness of the pack ice generation method proposed in this study.

4 Numerical results

4.1 Ship resistance

The total resistance, open-water resistance and ice resistance are predicted and validated against model

test data[19]. Ice resistance represents the time-averaged longitudinal contact force between the ship and ice, while total resistance is the sum of open-water resistance and ice resistance. The simulation conditions are identical to those in the model test, where the ice concentration C is 60% while the ship speeds U are 0.537 m/s, 0.690 m/s, 0.997 m/s and 1.304 m/s, with the corresponding Froude numbers Fr are $U/\sqrt{gL_{pp}}$= 0.077, 0.099, 0.142 and 0.186, respectively.

Fig. 6 shows the time histories of ship-ice longitudinal contact force at different ship speeds. It can be observed that the time histories exhibit significant fluctuations, which are related to the randomness and uncertainty of ship-ice collisions. Additionally, it can be noted that the extreme values of longitudinal contact force fluctuations at high ship speeds are larger than those at low ship speeds, indicating that as ship speed increases, the intensity of ship-ice collisions increases.

Fig. 7 shows the comparison of total resistance obtained by model test and numerical simulation; and Fig. 8 shows the comparison of open-water resistance and ice resistance obtained by model test and numerical simulation. It can be seen that the total resistance, open-water resistance and ice resistance calculated by CFD-DEM method agree well with the model test data, indicating that the numerical model proposed in this study has good accuracy in predicting ship resistance.

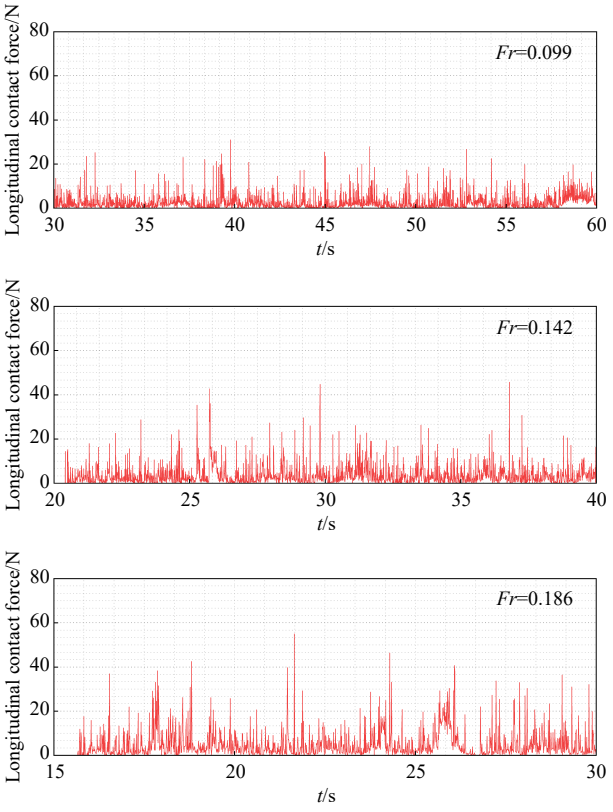

Fig.6 Time histories of ship-ice longitudinal contact force at different ship speeds

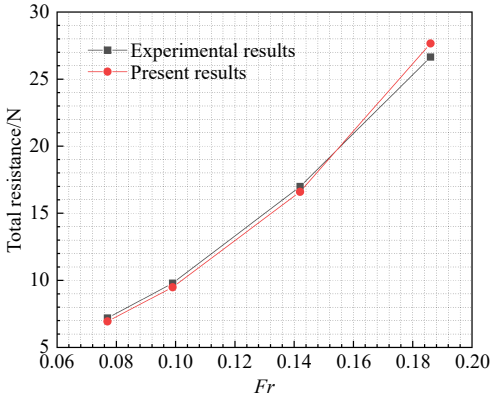

Fig.7 Comparison of numerical and experimental total resistance

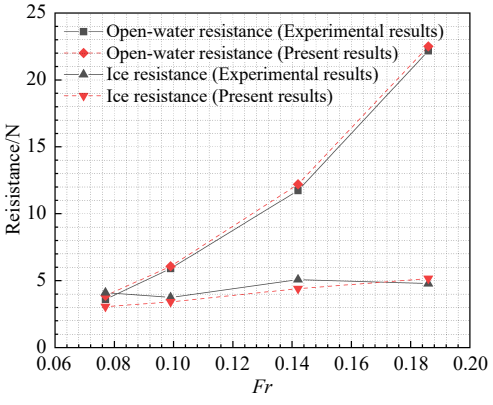

Fig.8 Comparison of numerical and experimental open-water resistance and ice resistance

4.2 Numerical phenomena

Fig. 9 illustrates the numerically simulated entire process of the ship navigating through the pack ice area at a speed corresponding to Fr = 0.186, and Fig. 10 shows the phenomena of ship-ice-water interaction. It can be observed that when the ship initially contacts the pack ice, the pack ice is affected by the bow waves,

leading to submergence and accumulation. As the ship navigates through the pack ice area, the motion state of the pack ice undergoes significant changes due to the ship-ice interaction and ship-generated waves within the exiting pack ice area, an ice-free channel is formed, with its width roughly equal to the ship breadth.

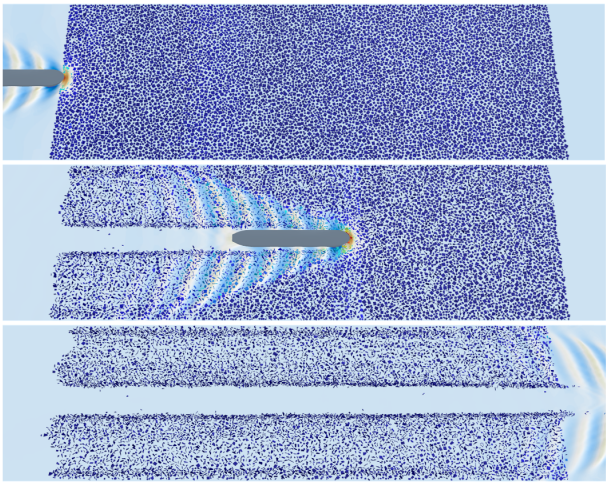

Fig.9 Simulated entire process of ship sailing through the pack ice area (Fr = 0.186)

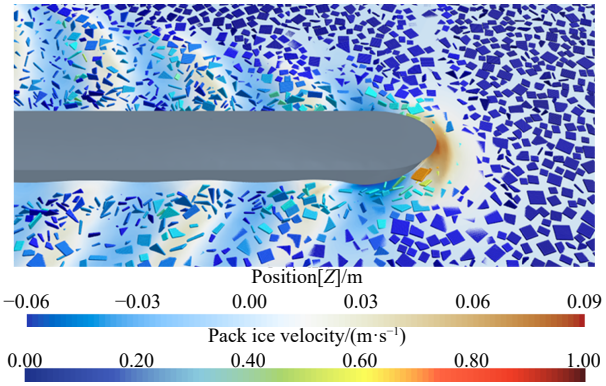

Fig.10 Simulated phenomena of ship-ice-water interaction (Fr = 0.186)

Fig. 11 shows a comparison of local phenomena between numerical simulation and model test. It can be seen that the numerical simulation fully captures the phenomena of the ship navigating in pack ice area. The simulated typical ship-ice interaction phenomena such as accumulation, sliding, and overturning of pack ice align well with those in the model test, indicating that the numerical model proposed in this study has a strong simulation capability.

Fig.11 Comparison of local phenomena between model test and numerical simulation （Fr = 0.077）

5 Concluding remarks

In order to address the limitations of existing numerical models and enrich the means of studying ship-ice-water interaction in pack ice area, distinct from the existing CFD-DEM models that assume the ship remains stationary, dynamic overset grid technology combined with DFBI to enable the free-running motion of the ship is employed in this paper. A numerical model for simulating a free-running ship navigating through the pack ice area and a high-precision pack ice generation method that can be used in conjunction with the numerical model are proposed. By comparing the numerical results with available model test data and experimental observations, the effectiveness of the proposed numerical model is verified. It is shown that this numerical model is capable of accurately predicting ship navigation resistance and simulating both the

overall process and local phenomena of ship navigation in pack ice region. Additionally, the model has strong potential and applicability in further studies. Based on this model, it is possible to conduct numerical simulation of ship self-propulsion and maneuvering motions in pack ice area in the future.

References

[1] Zhou L, Riska K, Von Bock und Polach F, et al. Experiments on level ice loading on an icebreaking tanker with different ice drift angles[J]. Cold Regions Science and Technology, 2013, 85: 79–93.

[2] Liu L, Ji S Y. Dilated-polyhedron-based DEM analysis of the ice resistance on ship hulls in escort operations in level ice[J]. Marine Structures, 2021, 80: 103092.

[3] Thomson J, Ackley S, Girard-Ardhuin F, et al. Overview of the Arctic Sea state and boundary layer physics program[J]. Journal of Geophysical Research: Oceans, 2018, 123(12): 8674–8687.

[4] Chen J, Kang S, Du W, et al. Perspectives on future sea ice and navigability in the Arctic[J]. The Cryosphere, 2021, 15(12): 5473–5482.

[5] Kim H S, Kim M C, Choi K S, et al. Full scale ice sea trials of Korean ice breaking research vessel 'Araon' on the big floes near Antarctica[J]. Journal of Marine Science and Technology, 2013, 18(4): 515–523.

[6] Jeong S Y, Choi K, Kim H S. Investigation of ship resistance characteristics under pack ice conditions[J]. Ocean Engineering, 2021, 219: 108264.

[7] Matala R, Suominen M. Investigation of vessel resistance in model scale brash ice channels and comparison to full scale tests[J]. Cold Regions Science and Technology, 2022, 201: 103617.

[8] Løset S. Discrete element modelling of a broken ice field - Part I: Model development[J]. Cold Regions Science and Technology, 1994, 22: 339–347.

[9] Wang C, Hu X H, Tian T P, et al. Numerical simulation of ice loads on a ship in broken ice fields using an elastic ice model[J]. International Journal of Naval Architecture and Ocean Engineering, 2020, 12: 414–427.

[10] Vroegrijk E. Validation of CFD+DEM against measured data[C]//Proceedings of the 34th International Conference on Ocean, Offshore and Arctic Engineering, Newfoundland, Canada, 2015.

[11] Huang L, Tuhkuri J, Igrec B, et al. Ship resistance when operating in floating ice floes: A combined CFD&DEM approach[J]. Marine Structures, 2020, 74: 102817.

[12] Zou M, Tang X J, Zou L, et al. Numerical simulation of ship-pack ice-water interaction and motion of pack ice based on CFD-DEM method[J]. IOP Conference Series. Materials Science and Engineering, 2023, 1288(1): 012019.

[13] Zhang J N, Zhang Y, Shang Y C, et al. CFD-DEM based full-scale ship-ice interaction research under FSICR ice condition in restricted brash ice channel[J]. Cold Regions Science and Technology, 2022, 194: 103454.

[14] Tang X, Zou M, Zou Z, et al. A parametric study on the ice resistance of a ship sailing in pack ice based on CFD-DEM method[J]. Ocean Engineering, 2022, 265: 112563.

[15] Xue Y Z, Zhong K, Ni B Y, et al. A combined experimental and numerical approach to predict ship resistance and power demand in broken ice[J]. Ocean Engineering, 2024, 292: 116476.

[16] Zou M, Tang X J, Zou L, et al. Numerical investigations of the restriction effects on a ship navigating in pack-ice channel[J]. Ocean Engineering, 2024, 305: 117968.

[17] Mucha P. Fully-coupled CFD-DEM for simulations of ships advancing through brash ice[C]//Proceedings of the SNAME Maritime Convention, Tacoma, WA, USA, 2019.

[18] Luo W Z, Jiang D P, Wu T C, et al. Numerical simulation of an ice-strengthened bulk carrier in brash ice channel[J]. Ocean Engineering, 2020, 196: 106830.

[19] Luo W Z, Guo C Y, Wu T C, et al. Experimental research on resistance and motion attitude variation of ship-wave-ice interaction in marginal ice zones[J]. Marine Structures, 2018, 58: 399–415.

[20] Timco G W, Weeks W F. A review of the engineering properties of sea ice[J]. Cold Regions Science and Technology, 2010, 60(2): 107–129.

[21] Zou M, Tang X J, Zou L, et al. Numerical simulation of a ship advancing in pack ice area based on CFD-DEM method[C]//Proceedings of the 42nd International Conference on Ocean, Offshore and Arctic Engineering, Melbourne, Australia, 2023.

碎冰中自由航行船舶的船–冰–水相互作用数值建模

邹　明[1a,2]，邹早建[1a,1b]，邹　璐[1a,1b]，朱圣涛[1a]

（1. 上海交通大学 a. 船舶海洋与建筑工程学院；b. 海洋工程全国重点实验室，上海 200240；2. 中国船舶及海洋工程设计研究院，上海 200011）

摘要：冰区航行船舶在极地运输和资源开采中发挥着关键作用。不同于现有的假定船舶静止的数值建模方法，本文采用动态重叠网格技术与 DFBI（Dynamic Fluid-Body Interaction）方法实现船舶的自由航行，提出一种可模拟船舶穿越碎冰域航行的数值模型。该模型应用 CFD（Computational Fluid Dynamics）方法求解流场，并采用 DEM（Discrete Element Method）模拟船–冰和冰–冰之间的相互作用。同时，本文还提出一种高精度的碎冰域生成方法，可与所提出的数值模型结合使用。通过将数值结果与模型试验数据及试验观测现象进行对比，验证了所提出数值模型的有效性，表明该模型在碎冰区航行船舶的阻力预报和航行过程数值模拟方面具有较强的能力，并具有良好的后续开发潜力和极区船舶碎冰区航行性能研究适用性。

关键词：碎冰；船–冰–水相互作用；CFD–DEM；动态重叠网格技术；船舶阻力

中图分类号：U661.31+1　　**文献标识码：**A

基金项目：水动力学全国重点实验室基金项目（2022-JCJQ-LB-028）

作者简介：邹　明（1995–），男，博士研究生；

邹早建（1956–），男，上海交通大学教授，博士生导师；

邹　璐（1983–），女，上海交通大学副教授，博士生导师；

朱圣涛（2000–），男，硕士研究生。